

Supplementary Information

A π -Stacked Pure Organic Material with Room Temperature

Phosphorescence

Yunzhe Zhou,^{a,c} Zhonghua Deng,^{b,c} Zhenyu Ji,^c Ziqing Zhang,^c Cheng Chen ^{*b,c} and Mingyan Wu^{*c}

^a College of Chemistry, Fuzhou University, Fuzhou, Fujian 350108, China.

^b Fujian Science & Technology Innovation Laboratory for Optoelectronic Information of China, Fuzhou, Fujian 350108, China

^c State Key Laboratory of Structural Chemistry, Fujian Institute of Research on the Structure of Matter, Chinese Academy of Sciences, Fuzhou, Fujian, 350002, China

Materials and Instrumentation:

All the solvents and reactants used were purchased from commercial companies without further purification except for specifying otherwise. ^1H NMR and ^{13}C NMR were recorded on a Bruker AV-400 spectrometer. Powder X-ray diffraction (PXRD) pattern was recorded on a MiniFlex diffractometer using Cu-K α radiation ($\lambda = 1.5406 \text{ \AA}$) at a scan speed of 2° min^{-1} . The X-ray diffraction data was collected on a Synergy Custom (Liquid MetalJet D2+) diffractometer, with Ga K α radiation ($\lambda = 1.34050 \text{ \AA}$). UV-Vis diffuse reflectance spectral measurements were carried out on a Perkin-Elmer Lambda 950 spectrometer using BaSO $_4$ as a reference. The photoluminescence spectra were determined by a FLS980 and FLS1000 fluorescence spectrometer at room temperature. The thermogravimetric analysis (TGA) was performed on a NETZSCH STA 449C unit at a heating rate of $10 \text{ }^\circ\text{C}\cdot\text{min}^{-1}$ under nitrogen atmosphere. Thin film test strips were prepared using polymethyl methacrylate (PMMA) as a polymer matrix.

Single-Crystal X-ray Crystallography:

The X-ray diffraction data for TPATA was collected on the Synergy Custom (Liquid MetalJet D2+) diffractometer, with Ga K α radiation ($\lambda = 1.34050 \text{ \AA}$). Absorption corrections were performed using a multi-scan method. The structure was solved by direct methods and was refined by the least-squares method with *SHELXL*-2016 program package. All non-hydrogen atoms were refined with anisotropic displacement parameters. Hydrogen atoms of the ligands were located by geometrical calculations, and their positions and thermal parameters were fixed during structural refinement. Structure refinement after modification of the data for the solvent molecules with the PLATON SQUEEZE program led to better refinement and data convergence.

Synthesis of 2,4,6-tris{4-[4-(diphenylamino)phenyl]phenyl}-1,3,5-triazine (TPATA):

2,4,6-Tris(4-Bromophenyl)-1,3,5-Triazine (2.00 g, 3.66 mmol), 4-(Diphenylamino)-Phenylboronic Acid (4.23 g, 14.64 mmol), Cs $_2$ CO $_3$ (4.98 g, 15.30 mmol) and Pd(PPh $_3$) $_4$ (0.6 g, 0.52 mmol) were added into one 500 mL schlenk flask containing 300 mL dioxane. The mixture was stirred at $90 \text{ }^\circ\text{C}$ for 72 h under nitrogen atmosphere. After the reaction was over, the resultant mixture was cooled down to room temperature and the solvent was removed under reduced pressure. The precipitate was purified by column chromatography to give TPATA (2.85 g, 75 %) as a yellow powder. Single crystal structure was obtained by recrystallization from dioxane. TPATA: ^1H NMR (400 MHz, CDCl $_3$): δ 7.10 (t, J=7.3, 6H), 7.15-7.25 (m, 12H), 7.32 (m, 12H), 7.62 (d, J=8.6, 6H), 7.81 (d, J=8.5, 6H), 8.86 (d, J=8.5, 6H).

Preparation of TPATA/PMMA film:

A series of TPATA/PMMA film were prepared by a drop-coating method using chloroform as solvent. The TPATA and PMMA powder were mixed at a w/w ratio of 1:1, and then dissolving in 5 mL of chloroform through ultrasonication.

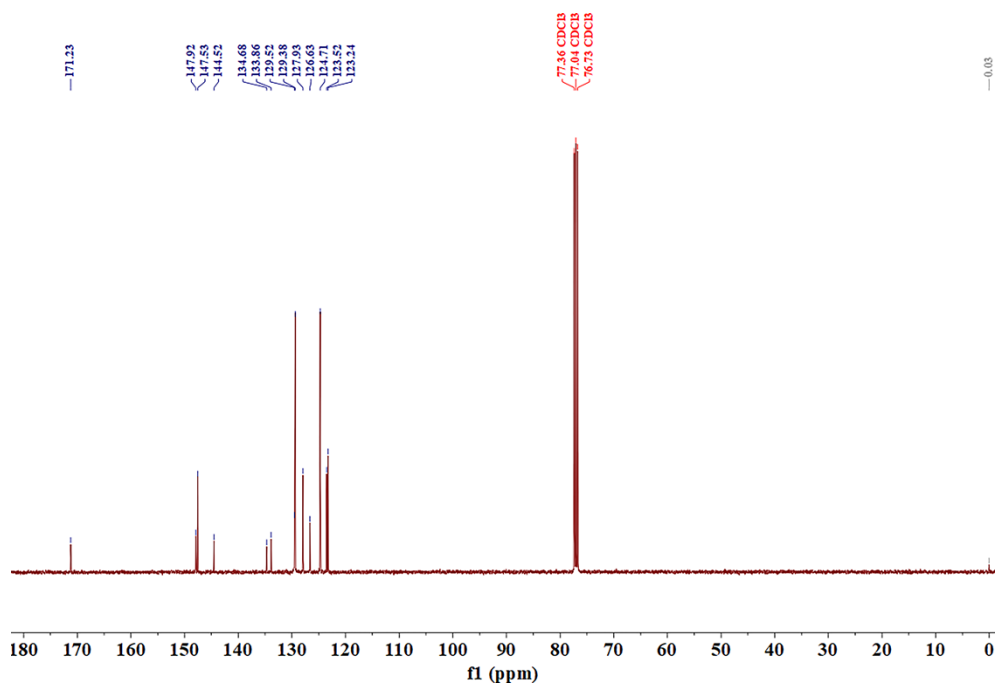


Fig. S2. ^{13}C NMR spectrum of compound TPATA.

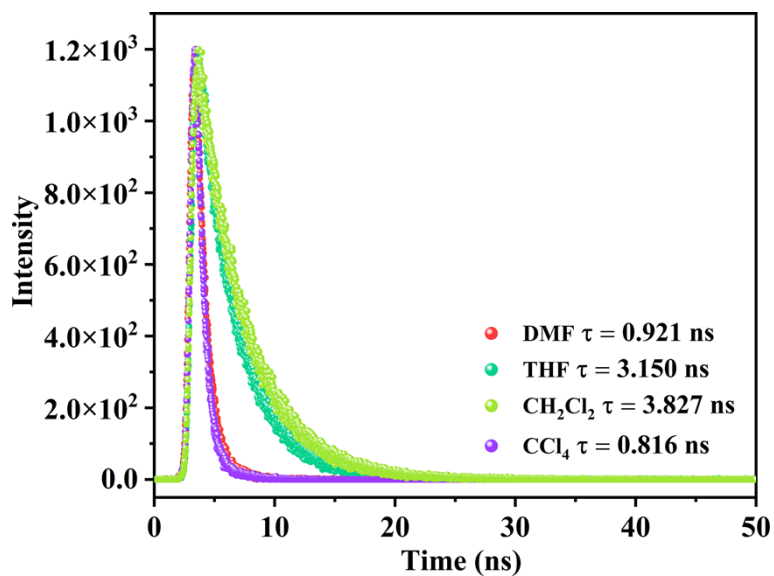


Fig. S3. Fluorescence decay curves of TPATA solution in CCl_4 , THF, CH_2Cl_2 and DMF. The fluorescence decay curves of TPATA solution in CCl_4 , THF, CH_2Cl_2 and DMF (the solvent polarity ranges from low to high) show the lifetime as 0.816, 3.150, 3.827 and 0.921 ns, respectively, which are consistent with the solvent polarity response rule of ICT state.

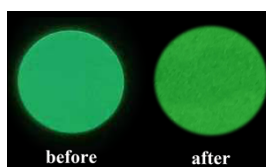


Fig. S4. Photographs of TPATA/PMMA films before and after exposure to CHCl_3 under a 365 nm UV lamp.

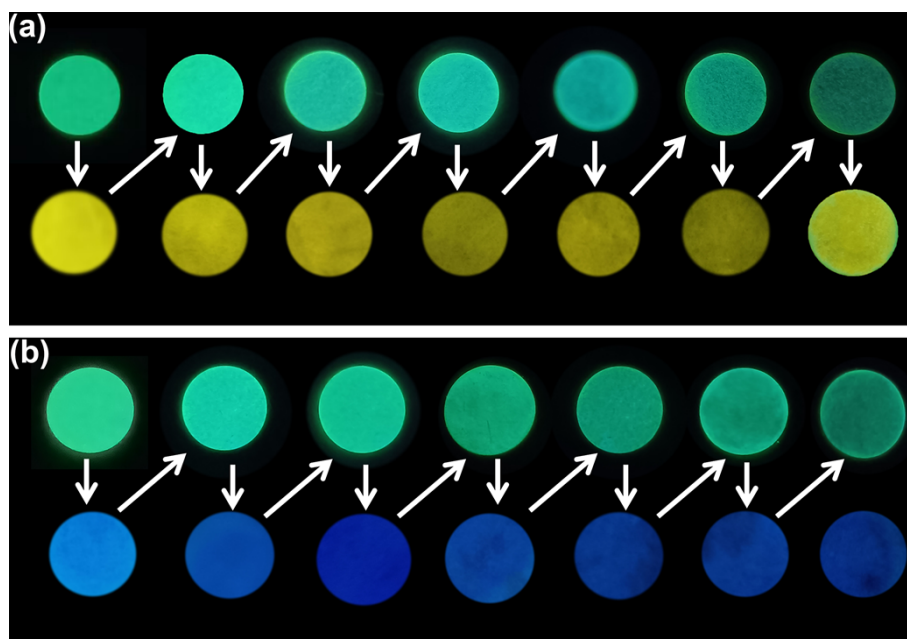


Fig. S5. Photographs of fluorescence changes on the TPATA/PMMA film before and after the exposure to CCl_4 (a) and CH_2Cl_2 (b) solvents under a 365 nm UV lamp for 7 cycles.

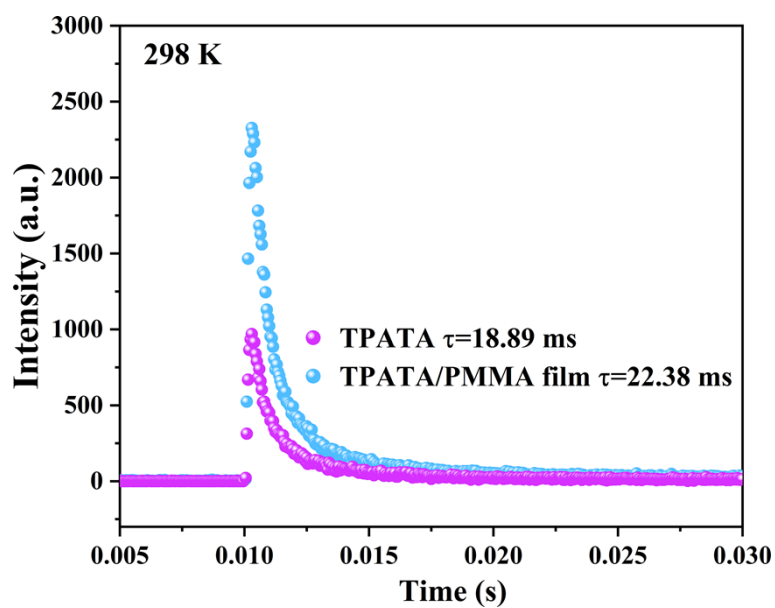


Fig. S6. Transient PL spectra of TPATA in crystals (pink) and TPATA/PMMA film (blue) at 298 K.

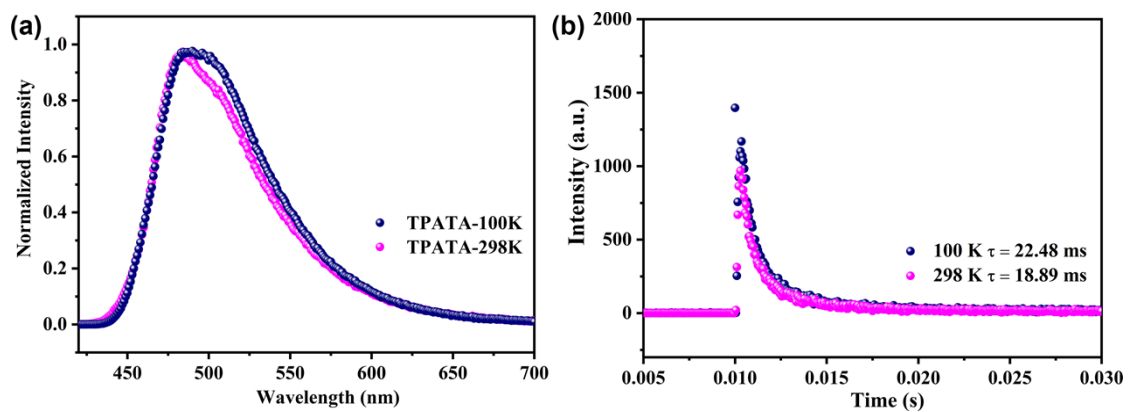


Fig. S7. (a) PL spectra of TPATA at 100 and 298 K (b) Time-resolved phosphorescence decay curves of TPATA at 100 and 298 K.

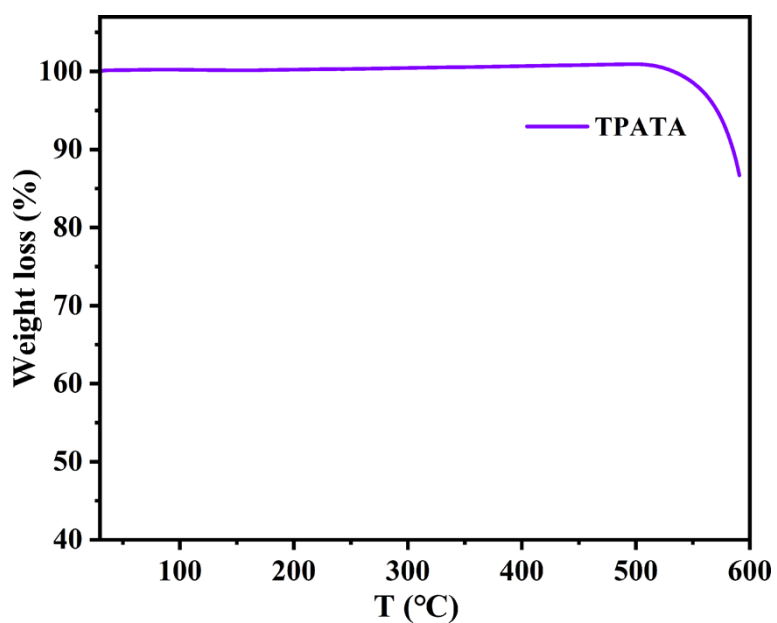


Fig. S8. TGA curve of TPATA.



Fig. S9. The optical microscope pictures of TPATA.

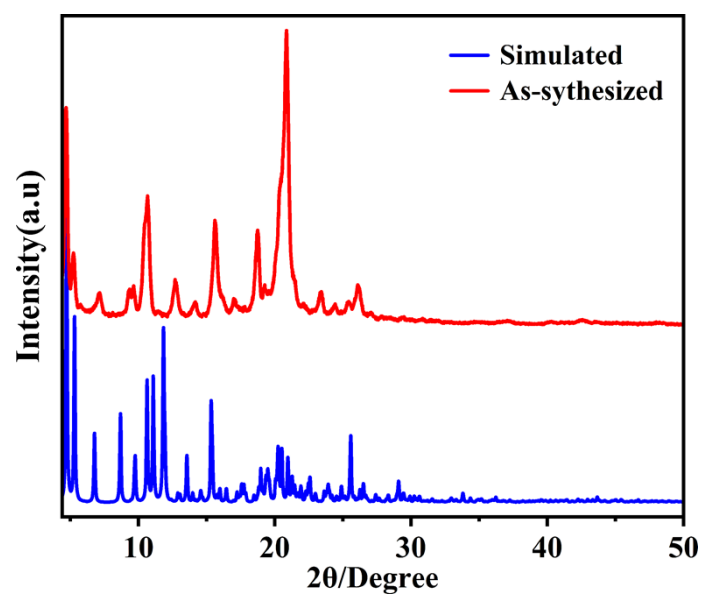


Fig. S10. The simulated and experimental PXR D patterns of TPATA.

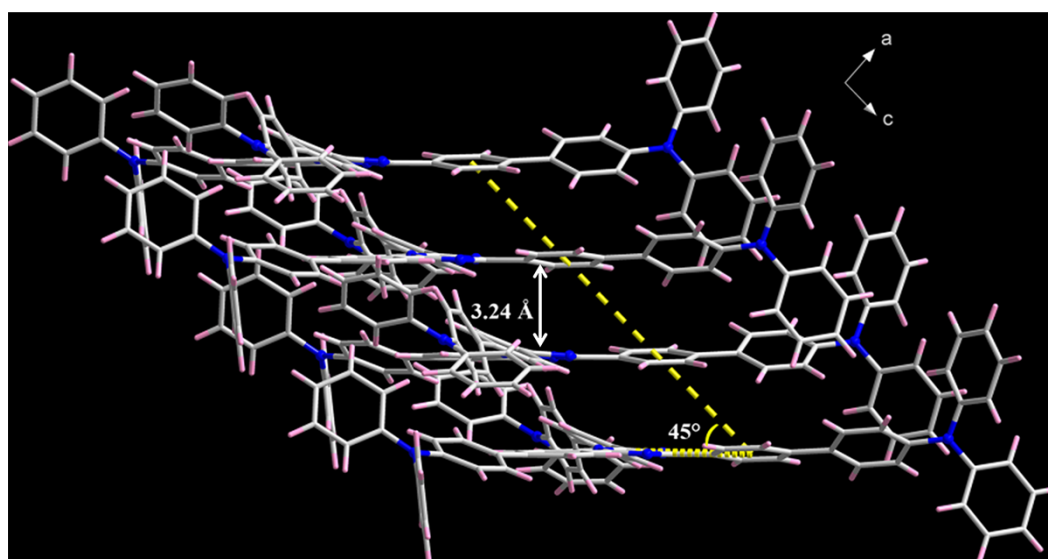


Fig. S11. Stacking fashion of TPATA molecules in the crystal structure (along *b*-axis).

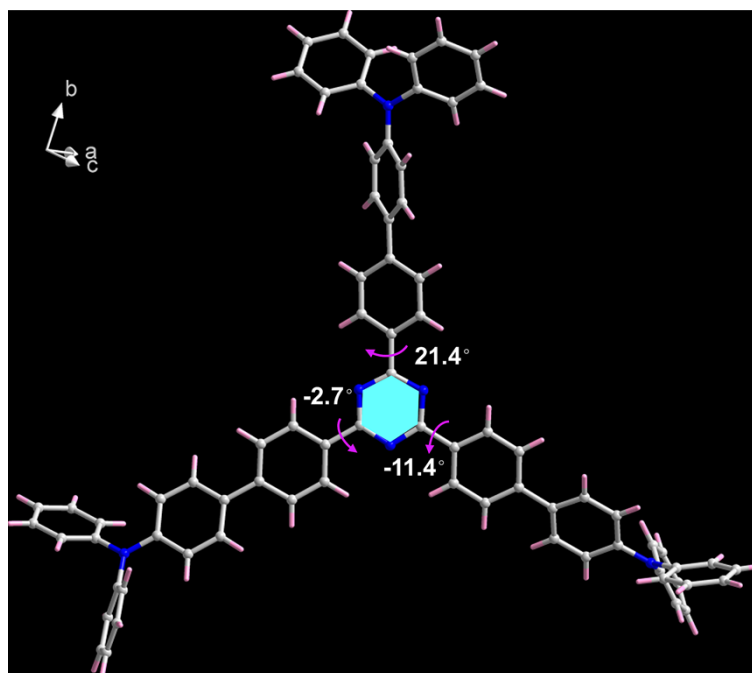


Fig. S12. The dihedral angles between triazine and the peripheral phenyl rings in the TPATA.

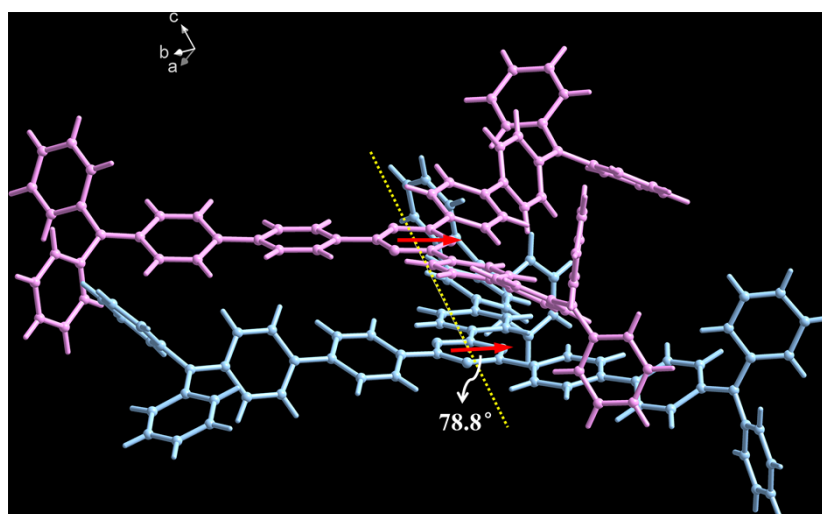


Fig. S13. Single-crystal structure of TPATA showing the formation of H-aggregates as evident by the measured angle (θ) of 78.8° between the transition dipoles and interconnective axis.

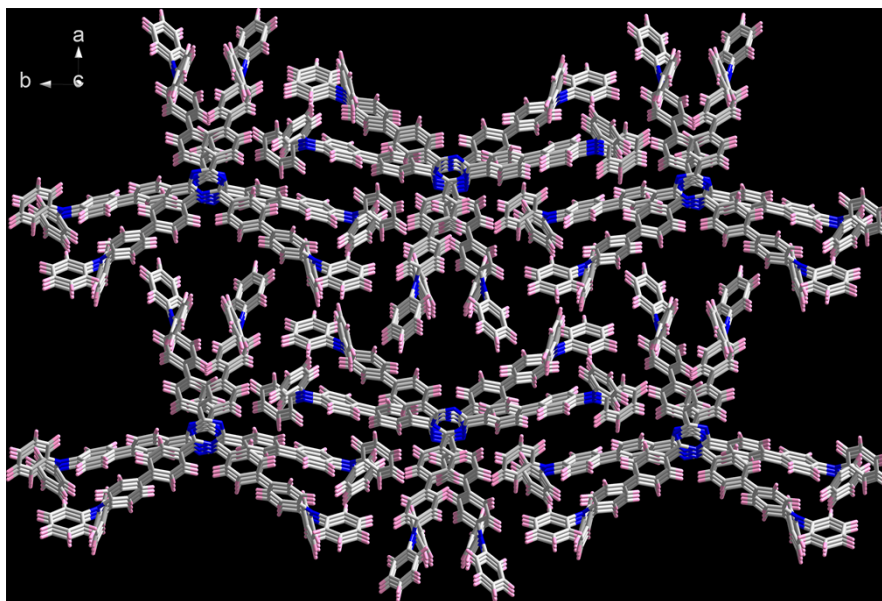


Fig. S14. Stacking structure of TPATA in the crystal (along *c*-axis).

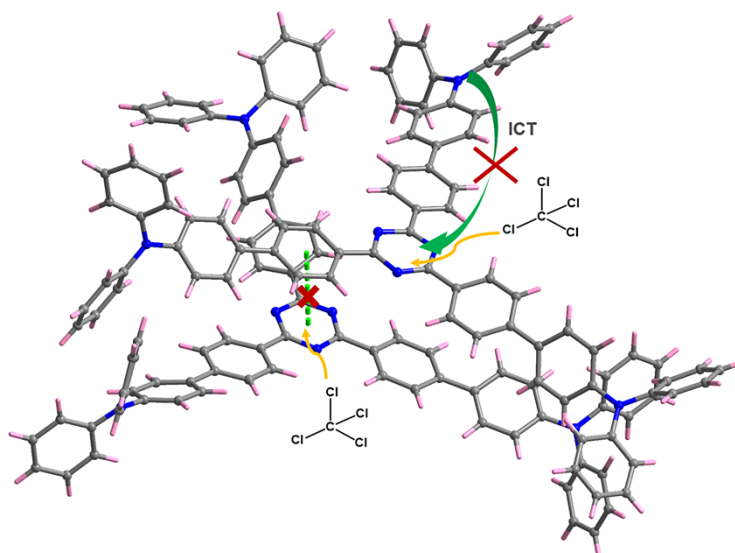


Fig. S15. Schematic diagram of halogenated solvent molecules blocking the intra-/intermolecular interactions. We speculate that the large response is due to an optimized fit of the solvent molecules incorporated into the crystal composite film, where the highly polarizable chlorine atoms interact strongly with the electron-deficient triazine ring. It causes the blocking of intramolecular ICT interactions and the intermolecular dipole-dipole interactions. It's worth noting that the CCl_4 molecule is full of chlorine atoms, and will cause the effective blocking of intra-/intermolecular interactions, which resulting the blue shifted of fluorescence. In contrast, CHCl_3 and CH_2Cl_2 molecules, which contain hydrogen atoms, are unable to completely block the intra-/intermolecular interactions, and thus exhibit fluorescence emission at longer wavelengths.

Table S1. Experimental data of photophysical properties of **TPATA** in different solutions.

Solvent	$\lambda_{\text{abs max}}$ (nm)	λ_{em} (nm)	Stokes shift (nm)
CCl₄	392	443	51
TOL	394	462	68
Diox	389	477	88
CHCl₃	393	514	121
EA	389	520	131
THF	392	523	131
CH₃CN	387	525	138
Butanol	390	534	144
CH₂Cl₂	393	546	153
ACE	390	586	196
NMP	400	594	194
DMF	395	604	209
DMSO	398	621	223

Table S2. Summary of crystal data and structure refinements for TPATA.

Compound	TPATA
CCDC	2245058
Empirical formula	C ₇₅ H ₅₄ N ₆
Formula weight	1039.24
T (K)	100
Crystal system	<i>monoclinic</i>
Space group	<i>P2₁/c</i>
<i>a</i> (Å)	18.76800
<i>b</i> (Å)	36.40600
<i>c</i> (Å)	9.54200
α (°)	90
β (°)	95.2700
γ (°)	90
V (Å ³)	6491.8(2)
Z	4
Radiation	GaK α
ρ_{calcd} (g/cm ³)	1.063
μ (mm ⁻¹)	0.062
F(000)	2184.0
Data / restraints / parameters	14344 / 0 / 730
Reflections collected / unique	49070 / 14344 [$R_{\text{int}} = 0.0704$]
Goodness-of-fit on F^2	1.076
Final R indices [$I > 2\sigma(I)$]	$R_1 = 0.0852$, $wR_2 = 0.3040$
R indices (all data)	$R_1 = 0.1195$, $wR_2 = 0.3321$
Largest diff. peak and hole	0.379 and -0.406 e.Å ⁻³

$${}^a R_1 = \sum \left| |F_o| - |F_c| \right| / \sum |F_o| \quad {}^b wR_2 = [\sum w(F_o^2 - F_c^2)^2 / \sum w(F_o^2)^2]^{1/2}$$